HHS Public Access

Author manuscript

Biochim Biophys Acta. Author manuscript; available in PMC 2016 April 12.

Published in final edited form as:

Biochim Biophys Acta. 2014 November ; 1842(11): 2060–2072. doi:10.1016/j.bbadis.2014.07.005.

A cytosolic protein factor from the naked mole-rat activates proteasomes of other species and protects these from inhibition

Karl A. Rodriguez[1,2], **Pawel A. Osmulski**[1,3], **Anson Pierce**[4], **Susan T. Weintraub**[6], **Maria Gaczynska**[1,3], and **Rochelle Buffenstein**[1,2,5,*]

[1]Sam and Ann Barshop Institute for Aging and Longevity Studies, University of Texas Health Science Center at San Antonio, 15355 Lambda Dr. San Antonio, TX 78245

[2]Department of Physiology, University of Texas Health Science Center at San Antonio, 7703 Floyd Curl Drive, San Antonio, TX 78229

[3]Department of Molecular Medicine, University of Texas Health Science Center at San Antonio, San Antonio, Texas, 15355 Lambda Dr. San Antonio, TX 78245

[4]Mitchell Center for Neurodegenerative Diseases, Department of Biochemistry and Molecular Biology. University of Texas Medical Branch Galveston, 301 University Boulevard, Galveston, TX, 77555

[5]Department of Cellular and Structural Biology, University of Texas Health Science Center at San Antonio, 7703 Floyd Curl Drive, San Antonio, TX 78229

[6]Department of Biochemistry and Director, Mass Spectrometry Laboratory, The University of Texas Health Science Center at San Antonio, 7703 Floyd Curl Drive San Antonio, TX 78229

Abstract

The naked mole-rat maintains robust proteostasis and high levels of proteasome-mediated proteolysis for most of its exceptional (~31y) life span. Here, we report that the highly active proteasome from the naked mole-rat liver resists attenuation by a diverse suite of proteasome-specific small molecule inhibitors. Moreover, mouse, human, and yeast proteasomes exposed to the proteasome-depleted, naked mole-rat cytosolic fractions, recapitulate the observed inhibition resistance, and mammalian proteasomes also show increased activity. Gel filtration coupled with mass spectrometry and atomic force microscopy indicates that these traits are supported by a protein factor that resides in the cytosol. This factor interacts with the proteasome and modulates its activity. Although HSP72 and HSP40 (Hdj1) are among the constituents of this factor, the observed phenomenon, such as increasing peptidase activity and protecting against inhibition cannot be reconciled with any known chaperone functions. This novel function may contribute to the exceptional protein homeostasis in the naked mole-rat and allow it to successfully defy aging.

[*]To whom all correspondence should be addressed: Rochelle Buffenstein, Barshop Institute, STCBM 2.2; 15355 Lambda Drive, San Antonio Texas, 78245. Phone: 210 562 5062 (RB), Fax: 210 562 5028, Buffenstein@uthscsa.edu.

Keywords

Proteasome; Heat Shock Protein; Naked mole-rat; Protease Inhibitor; Protein degradation; Aging

1.0 INTRODUCTION

The longest-lived rodent, the naked mole-rat, *Heterocephalus glaber,* lives nearly an order of magnitude longer than similar-sized mice (1). Despite high levels of oxidative stress evident even at young ages (2), naked mole-rats maintain cancer-free good health and reproductive potential well into their third decade of life (3). Furthermore, these rodents show pronounced *in vivo* and *in vitro* resistance to a wide spectrum of toxins including oxidative stressors, heavy metals, and chemotherapeutics (4,5). This is also evident at the macromolecular level with mole-rat proteins markedly resistant to both oxidative damage and unfolding stressors (6). This generalized resilience against stress is likely due to efficient maintenance of protein quality control, involving both proteolytic machinery to remove damaged proteins and molecular chaperones [HSPs] that assist in protein repair or elimination.

HSPs bind to exposed hydrophobic regions of proteins preventing their aggregation and promoting their correct folding (7,8). If the process is unsuccessful, HSPs direct protein removal via either the ubiquitin proteasome system [UPS] or autophagy. The UPS degrades the majority of intracellular proteins and is considered pivotal for the digest of oxidatively damaged substrates (7,9). Proteolysis of damaged proteins occurs primarily in the cytosol (10,11). Here, ubiquitinylated, misfolded, oxidized, or otherwise damaged proteins are recognized by the proteasome (12) and cleaved into peptides by active centers located in the proteasome 20S catalytic core (10). The active proteolytic centers display three major specificities designated chymotrypsin-like [ChT-L], trypsin-like [T-L], and post-glutamyl, peptide-hydrolyzing [PGPH], reflecting the divergent chemical properties of the amino acid residues on the carboxyl side of the scissile bond (10).

Stress resulting from protein damage challenges both HSPs and the UPS by firstly increasing the load of substrates destined for degradation, and secondly by directly damaging the proteasome and thereby impairing its function (9). Indeed, the reported decline in mouse proteolytic degradative capacity with age is attributed to the stress induced increase in misfolded protein load and accompanying reduction in proteasome efficiency (9,13,14). In contrast, proteasome activity in aged naked mole-rats, like that in the cells of supercentenarians (15), remains at high levels even though these rodents from an early age bear a greater burden of proteotoxic stress from oxidatively-damaged proteins (6). We postulate that as this species evolved mechanisms to prevent damage from both the barrage of endogenous and environmental stressors, they developed better maintenance of somatic integrity and proteostasis and thereby longer lives.

RNA sequence analysis [RNA-Seq] reveals that many of the genes involved in the regulation of UPS as well as those of HSPs are detected at much higher levels in the naked mole-rat relative to mice (16,17). However, the particular expression pattern of UPS components as well as HSPs can only partially explain the high and sustained levels of proteasome activity in the naked mole-rat, such that young mole-rats exhibit five-fold higher specific peptidase

activities compared to physiologically aged mice (18). Moreover, RNA-Seq data do not explain the resilience of naked mole-rat proteasomes to competitive inhibitors (6,19). Although published studies have documented that proteasome activity may be elevated in response to mild oxidative challenge (9,20), to date there has been no report of resistance of proteasomes to inhibition (20). We hypothesize that the naked mole-rat employs novel molecular mechanisms to protect proteasome function and achieve sufficiently high levels of catalytic activity necessary to effectively maintain proteostasis.

2. MATERIALS AND METHODS

2.1 Animals

This study used two similarly sized physiologically age-matched rodent species namely *Mus musculus* (C57BL/6 mice; 4–6 months) and *Heterocephalus glaber* (naked mole-rats; 2–3 years). The mice were fed a standard NIH-31 chow *ad libitum* and maintained in cohorts of four animals in microisolator mouse cages at 25°C, on a 12-h dark/light cycle. Naked mole-rats were from the well-characterized colonies of Dr. Rochelle Buffenstein housed at the University of Texas Health Science Center, San Antonio (3). Naked mole-rats were housed in simulated, multi-chambered burrow systems under constant climatic conditions that aimed to approximate their native habitat (30°C; 30–50% RH). Naked mole-rats were given an *ad libitum* supply of fresh fruits and vegetables supplemented weekly with a high protein and vitamin enriched cereal (Pronutro, South Africa). In this study, female mice were used to correspond with past studies undertaken in this field by our lab (13). As the subordinate naked mole-rats are sexually monomorphic (21), and we found no sex specific differences in any of our measurements we used tissues from both male and females (18).

Animals were anesthetized with isofluorane, euthanized by cardiac exsanguination and the liver tissue immediately excised and flash frozen in liquid nitrogen. All procedures involving animals were approved by the Institutional Animal Care and Use Committee at the University of Texas Health Science Center (San Antonio, TX)

2.2 Whole Tissue Lysates and Subcellular Fractionation

Mouse and naked mole-rat liver lysates were separated into cytosolic, microsomal, and nuclear fractions using a modified Millipore Corp. procedure as previously described (13,18). These various fractions were then used in peptidolytic assays.

2.3 Peptidolytic Assay

Proteasome activity was measured using fluorogenic model peptide substrates (Boston Biochem, Boston, MA) specific for the ChT-L and T-L active centers of the proteasome as previously described (18). Parallel activity assays were performed with varying concentrations of proteasome inhibitors that represented four different classes of compounds with distinct modes of inhibitory action. These compounds modify active centers using a boronate group (bortezomib [BZ] (Sigma-Aldrich, St. Louis, MO)); an aldehyde (N-(benzyl-oxycarbonyl) leucinyl-leucinyl-leucinal [MG132]); a vinyl sulfone, (adamantane-acetyl-(6-aminohexanoyl)$_3$-(leucinyl)$_3$-vinyl-(methyl)-sulfone [Adh (VS)]); or a lactone (lactacystin [LC] (Calbio-chem/EMD Millipore, Billerica, MA)). Concentrations ranged from 5nM to

10μM for BZ, 0.2μM to 8μM for LC, and 10μM to 250μM for MG132 and Adh(VS) based on determinations from previous studies (13,18,22,23). Specific peptidolytic activity was presented as pmol of released AMC in 1 min per 1 μg of total protein in the test sample. This was determined after generating a standard curve using serial dilutions of 1mM AMC and measuring the fluorescence using a Spectra-Max Multi-mode microplate reader (Molecular Devices, Sunnyvale, CA) as previously described (18).

The IC_{50} concentration was determined as the concentration of inhibitor that reduced proteasome activity by 50%. For that purpose exponential decay or sigmoidal functions were fitted to the titration data and the corresponding IC_{50} extracted (OriginPro, OriginLab Corp or CompuSyn).

2.4 Crossover Assays

A partial proteasome purification of five separate naked mole-rat and five mouse samples was performed using high-speed centrifugation (27,28). Briefly, the samples were centrifuged at 100,000xg in an S120 AT-2 (Sorvall) rotor for 5 hours. The supernatant was decanted and pooled, while the pellet was re-constituted in 50mM Tris, pH 7.4 containing 20% glycerol and 1mM DTT. The pellet was left on ice for 30 minutes and then centrifuged again for 5 minutes at 16,000xg. Protein content was measured using the BCA Protein Assay Kit (Pierce, Thermo Scientific, Rockford, IL, USA) and the peptidolytic assay for ChT-L activity described above was performed starting with a 1:1 ratio of mouse or naked mole-rat purified proteasome to naked mole-rat or mouse pooled supernatant. We also performed these experiments using purified human 26S proteasome and yeast 20S proteasome (Enzo Life Sciences, Plymouth Meeting, PA, USA). Parallel with these samples, supernatants alone, and original mouse and naked mole-rat cytosolic fractions were tested on the same 96-well plate used for the assay.

2.5 Size-exclusion spin filtration

The size-exclusion filtration procedure was performed according to the manufacturer's instructions (Amicon Microcon ultracel YM-3 cellulose filter, 3000Da) (EMD Millipore, Billerica, MD, USA). Briefly, 500 μL of supernatant prepared as described under "Crossover Assay" was placed on the filter and spun at 14,000xg for 30 minutes (3 x 10 minute washes). The filtrate was collected and then the sample reservoir was upended, and spun for 3 minutes at 14,000xg to collect the retentate. Protein content was measured using the BCA Protein Assay Kit (Pierce, Thermo Scientific, Rockford, IL, USA) and ChT-L activity was measured as described previously using a 1:1 mouse or naked mole-rat purified proteasome to naked mole-rat pooled supernatant, retentate, or filtrate.

2.6 Atomic Force Microscopy (AFM) Imaging

Chromatographic fractions showing inhibition resistance (see below), purified human 20S proteasome, and their mixture were subjected to AFM imaging with tapping (oscillating) mode in liquid using the Multimode Nanoscope IIIa AFM (Bruker) as previously described (24). Briefly, 3 μL of sample containing 2 ng of h20S or undiluted fr. 23, or a mixture of both, were deposited on freshly cleaved muscovite mica and left for 2–3 min. at room temperature to allow for electrostatic binding to mica. Then, the sample was overlaid with

30 μL of imaging buffer (5 mM Tris/HCl, pH 7.0), and subjected to AFM imaging. Oxide-sharpened silicon nitride tips on cantilevers with a nominal spring constant 0.32 N/m mounted in the wet chamber (Bruker Corp.) were used for imaging. The resonant frequency was tuned to 9–10 kHz, with a drive voltage of 200–500 mV. To minimize "tapping" force interference with the imaging molecules, relatively high values of the set point, 1.5 V to 1.9 V, were applied. Fields of 0.56 μm^2 to 1 μm^2 were scanned at a rate of 3.05 Hz with trace and retrace images collected with a resolution of 512 x 512 pixels. The images were processed only with the standard plane-fit and flattening; therefore they should be considered as "raw". For display purposes the brightness and contrast of the images was adjusted and the occasional scan lines were removed with the Nanoscope software. Morphometric analysis of particles was performed with the grain analysis function in SPIP software (Image Metrology). To detect distinct classes of particles, the Peak Analyzer function was applied to the footprint area of all particles followed by hierarchical cluster analysis executed on footprint area, height, aspect, perimeter, and fiber length as unique and independent morphometric parameters (OriginPro). A new class of objects characterized by the set of identified morphometric parameters representing complexes of resistasome with 20S proteasome was then sourced to the specific objects in the original AFM images. As a self-test, the method correctly identified the top view and side view proteasomes in samples containing only 20S particles and in the mixture with fr. 23.

2.7 Multiplex Western Blot Analysis of Heat Shock Proteins

Tissue lysates or sub-cellular fractions were separated in 12% SDS-PAGE (Biorad Life Sciences, Hercules, CA) and transferred to nitrocellulose membranes (Biorad Life Sciences, Hercules, CA). The membranes were probed with antibodies against the following proteins: HSP110 (rabbit, SPA-1101, 1:5k), HSP90 (mouse, SPA831, 1:20K), HSP70/72 (mouse, SPA810, 1:10K), HSP40 (HDJ1) (rabbit, SPA400, 1:2.5K), HSP25/HSPB1 (rabbit, SPA801, 1:10K), (Enzo Life Sciences, Plymouth Meeting, PA, USA). We also used antibodies against HSC70 (mouse, sc-7298, 1:10K) (Santa Cruz Biotechnology, Santa Cruz, CA, USA). Blots were stained with Ponceau-S to measure total protein load. Primary antibodies were detected using anti-mouse IRDye 680LT, or anti-rabbit IR Dye800 CW (Li-Cor) conjugated antibodies. Secondary antibodies were incubated at 1:10K (anti-rabbit) or 1:20K (anti-mouse) for 2 hours at room temperature and images were captured using the Odyssey Imaging System (Li-Cor, Lincoln) for IRDye 680LT, IR Dye800. Immunoblots were quantified using the ImageJ public domain Java image processing program (http://rsbweb.nih.gov/ij/).

2.8 Gel Filtration Chromatography

The 5-hr supernatant was fractionated with gel filtration chromatography on a Superose 6 GL 10/30 column (GE Healthcare) fitted into a BioCad Sprint (Perseptive Biosystems) HPLC. A 100μL sample of approximately 2μg/μL protein concentration was loaded. Chromatograms were developed with a column buffer (50mM Tris/HCl pH 7, 20% glycerol) using 0.4mL/min flow rate. The volume of collected fractions was 500μL. About 48 fractions per a single chromatogram were collected. Fractionation progress was monitored with absorption readings at 260 and 280nm. The apparent molecular weight of separated

proteins was determined based on elution volumes of a set of gel filtration markers (Bio-Rad) ranging from 1,350 (vitamin B12) to 670,000 Da (bovine thyroglobulin).

Concentration of protein in fractions was determined with a BCA assay (Pierce, Thermo Scientific, Rockford, IL, USA). Fractions were concentrated as necessary using a Centricon 3000Da cutoff filter (Amicon Microcon ultracel YM-3 cellulose filter; see Size Exclusion Column above; EMD Millipore, Billerica, MA, USA) and the peptidolytic assay for ChT-L activity was performed as described above (see Peptidolytic Assay, main and supplementary text) with 0 and 20μM of MG132.

2.9 *In vitro* Depletion Assays

Anti-HSP72 (Enzo, SPA-810), anti-HSP40 (Hdj1) (Enzo, SPA-400), anti-HSP25 (Enzo, SPA-801), or anti-HSP90 (Enzo, SPA831) specific anti-bodies were added in increasing concentrations ranging from 10pg to 400pg (made as serial dilutions from the original stock using PBS with 50% glycerol) to either naked mole-rat cytosolic lysates or naked mole-rat supernatants separated from these lysates (see Crossover Assays above). Because of the sequence similarity between mice and naked mole-rats of the key chaperones measured in this study, it was assumed that the antibodies could recognize the targeted protein in each species. For chemical inhibition of HSP72, increasing concentrations of VER155008 (25nM to 1000nM, Tocris Bioscience, UK) and pifithrin-μ (10μM to 1000μM; both Calbiochem/EMD Millipore, Billerica, MA USA) were added to lysates or supernatants in this manner. Next, the mixture was incubated at 30°C for 1hr in the presence of 1mM ATP. Immediately, the antibodies or small-molecule inhibitors and purified human 26S proteasome or 5hr-naked mole-rat partially purified proteasome as necessary were added to the sample mixture. Then ChT-L activity was tested as described above using Suc-LLVY-AMC in the presence or absence of 20μM of MG132.

2.10 Immunoprecipitation Assay

Immuoprecipitation was performed with the Protein A/G PLUS-Agarose Immunoprecipitation Reagent (Santa Cruz Biotechnology, Santa Cruz, CA) using the protocols suggested by Enzo (www.enzolifesciences.com/support/antbodies/protocols/immunoprecipitation-protocol/) with 1μg of anti-HSP70/72 antibodies (Enzo, SPA-801) per 100μL of mouse or naked mole-rat liver lysates (final concentration 1mg/mL).

After an overnight incubation at 4°C of the immune complex, the protein A/G beads were added and incubated for 2hrs at 4°C. The beads were collected by microcentrifugation, washed 5X with PBS, resuspended in 2X Laemmli reducing running buffer (4% SDS, 20% glycerol, 10% 2-mercaptoethanol, 0.004% bromophenol blue, 0.125M Tris HCL; 95°C for 5 min) and then subjected to SDS-PAGE separation under de-naturing conditions. The gels were transferred to PVDF membrane and then tested with the same antibodies against HSP90, HSP72, HSP40, and HSP25 used in previous Western blots and antibodies for proteasome subunits, RPT5 (Enzo, mouse PW8770, 1:2K), and α7 (Enzo, mouse PW8110, 1:5K). HRP-conjugated secondary antibodies for goat, rat, or rabbit (Santa Cruz) were used to visualize the immuno-reaction using the ECL Prime Western Blotting Detection Reagent,

a chemiluminescent substrate (Amersham, Buckinghamshire, UK). Immunoblots were visualized using the Typhoon 9410 variable mode imager or on x-ray film (GE Healthcare).

2.11 Protein Identification with Mass Spectrometry

Proteins were separated by 1-D SDS-PAGE and proteins in each gel lane were digested *in situ* with trypsin (Promega). The digests were analyzed by capillary HPLC electrospray ionization tandem mass spectrometry (HPLC-ESI-MS/MS) on a Thermo Fisher Orbitrap Velos mass spectrometer. The MS data were searched against the rodent subset of the NCIBnr protein database (NCBInr_20130102; 316,972 sequences) by Mascot (Matrix Science). The Mascot results were subjected to a subset search by X! Tandem followed by determination of probability assessments of the peptide assignments and protein identifications by Scaffold (Proteome Software).

2.12 Statistical Analysis

A two-tailed Student's t-test on two different statistical platforms (Microsoft Excel 2010; SigmaPlot) was used to determine significant differences in the means for the peptidolytic assays and Western blot quantitation. One-way ANOVA was used in the inhibition resistance experiments to analyze the variances between species and fractions while two and three-way ANOVAs were used to test variance when comparisons between treatments, species, and concentration were necessary (SigmaPlot). Statistical significance was set at the $p < 0.05$ level. All pairwise multiple comparison procedures used the Bonferroni and Holm-Sidak corrections to counteract the probability of false positives.

3. RESULTS AND DISCUSSION

3.1 Naked mole-rat proteasomes are resistant to proteasome inhibition

To test this hypothesis, we measured proteasome activity in the various subcellular fractions of liver lysates of mice and mole-rats when treated with several proteasome-specific small molecule inhibitors, namely MG132, [Adh(VS)] (25), [BZ] (22), and LC (23). These well-characterized competitive inhibitors bind to the proteasome catalytic centers using distinct chemical mechanisms. ChT-L activity is the primary target for all four inhibitors. BZ, an approved anti-cancer drug (26,27), is regarded as the most specific for this peptidase activity. T-L activity is known as a secondary target for both MG132 and LC (23), and Adh(VS) inhibits all three peptidases with relatively similar efficiency. We compared these peptidase activities in untreated and inhibitor-treated samples. In sharp contrast to data acquired with mouse proteasomes, we found that naked mole-rat proteasomes from cytosolic extracts maintained ChTL activity when treated with specific competitive proteasome inhibitors, (Figure 1). Remarkably, naked mole-rats required 10-fold higher concentrations to ablate 50% of ChT-L activity (the IC_{50}) for both MG132 and LC while the IC_{50} for Adh(VS) was 22-fold greater (Figure 1; Table 1). Strikingly, the ChT-L IC_{50} concentration for BZ was more than two orders of magnitude (163-fold) higher in the naked mole-rat than in mouse cytosolic extracts (Figure 1; Table 1). T-L activity also showed inhibition resistance to MG132 and Adh(VS) with the T-L IC_{50} 5-fold greater in naked mole-rats compared to mice for both agents (Figure 2A; Table 1).

Inhibition resistance was restricted to the cytosolic fraction since it was not observed in the microsomal or nuclear fractions of either species (Figure 2B; Table 1). Since the cytosolic fraction is most likely to encounter cellular stressors, we concluded that cytosol-specific resistance to proteasome inhibition observed in the naked mole-rat could be an important component of the cytoprotective arsenal that underlies naked mole-rat resilience against potentially harmful conditions (5).

3.2 Proteasome resistance is transferrable among species

To evaluate whether the observed resistance to inhibition was an intrinsic property of the naked mole-rat proteasome or is rather mediated by specific factors within the intracellular milieu, we used a simple “cross-over” experimental design (Figure 3A). Mole-rats and mice proteasomes were partially purified from the cytosolic fractions using differential centrifugation (28,29) and the proteasome-enriched pellet and the proteasome-depleted supernatant were separately retained. The supernatant of both species had very low ChT-L activity (Figure 3A, bar G) confirming efficient removal of proteasomes from the cytosol. As a next step, ChT-L activity was measured in the “reconstituted cytosol” containing proteasome-depleted (SN) plus proteasome-enriched (Prot) preparations from either species in a 1:1 ratio of the original protein contents. When the $Prot_{NMR}$ was resuspended in SN_{Ms}, it no longer showed resistance to MG132, and also exhibited similar proteasome specific activity to that observed in mouse lysates (Figure 3A, bars C, F). Conversely, $Prot_{Ms}$ activity more than doubled upon mixing with the SN_{NMR} (Figure 3A, bar F). Furthermore, the $Prot_{Ms}$, when incubated in SN_{NMR}, became resistant to inhibition thus mirroring the cytosolic proteasome activity profile of naked mole-rat (Figure 3A, bar C). These data reveal that both elevated proteasome activity of naked mole-rats and inhibition resistance are not due to intrinsic proteasome properties conferring a more stable and more efficient proteasome, but rather, are due to protective modulators of proteasome activity within the cytosolic milieu.

We found that the cytosolic milieu not only modulated mouse proteasome activity but that the SN_{NMR} also conferred these same effects on both human and yeast proteasomes. When we exposed purified human 26S or yeast 20S proteasome to the SN_{NMR} we noticed an enhanced resistance to BZ inhibition (Figure 3B,C). Indeed levels of proteasome activity and inhibition resistance, when treated with SN_{NMR} in these evolutionarily divergent species, converged to that observed in naked mole-rats. Moreover, exposure of human 26S to increasing concentrations of SN_{NMR} resulted in a systematic increase of ChT-L activity and inhibition resistance (Figure 4A). In contrast, the treatment with SN_{MS} resulted in trivial increases in ChT-L activity at only the highest ratio of SN_{MS} to human 26S proteasome [h26S], and no inhibition resistance at any concentration of SN_{Ms} (Figure 4A). These data provide strong evidence that components within the naked mole-rat cytosol protect its proteasome from agents that commonly impair proteasome function. This cytosolic factor is transferrable to other species and capable of inducing similar protective and modulatory effects.

Both partially purified mouse proteasomes and purified human 26S also showed marked increases in specific proteasome activity even in the absence of chemical inhibition (Figure

3A,B). The mechanism(s) facilitating this increase in activity are unknown and possibly modulation of proteasome activity in the absence of inhibitory agents may be a mammal-specific property for this was not evident when yeast 20S proteasomes where incubated with SN_{NMR} (Figure 3C). It is intriguing that at least the inhibition resistance conveyed by the naked mole-rat cytosolic factor is universal from yeast to mammalian proteasomes.

3.3 Identification of the naked mole-rat activation/resistance factor

We tested if the observed changes in proteasome function in the presence of the SN_{NMR} were conveyed by small molecules or specific macromolecule(s) that directly interact with the proteasome and alter its properties. The involvement of cytosolic “small molecules” was ruled out by evaluating proteasome activity and inhibition resistance in the presence of the flow-through (i.e., metabolites, small peptides; Figure 4B) or retentate (proteins and other macro-molecules) after the 3-kDa cutoff spin filtration of cytosols. When the mouse or naked mole-rat proteasome was exposed to the retentate, it also exhibited a similar degree of inhibition resistance to that observed when it was exposed to the SN_{NMR} in the cross-over experiment (Figure 4B; Table 2). However, when proteasomes were treated with filtrate alone, the resistance was not observed (Figure 4B; Table 2). Interestingly, when we fractionated the supernatant with a 100-kDa cut-off filter and then measured the peptidolytic activity in the presence of the flow-through, the inhibition resistance capability was removed suggesting that this feature of the cytosolic factor was facilitated by a molecule or a group of molecules larger than 100 kDa (Figure 4B). To rule out sequestration of the inhibitors or their degradation in the supernatant, we pre-incubated BZ with SN_{NMR}, SN_{Ms} and buffer alone. Then, we recovered the BZ by spin filtering each sample through a 3-kDa cutoff membrane. Next, we tested ChT-L activity of human 26S proteasome treated with the obtained filtrates. All three samples apparently contained highly potent BZ (Figure 4C), therefore we concluded that the inhibitor is not substantially degraded, modified or sequestrated by components of the supernatant.

Based upon these results we hypothesized that both proteasome activation and inhibition resistance are conferred by cytosolic proteins. To assess this we subjected both mouse and naked mole-rat lysates to heat stress for 1hr at temperatures ranging from 32°C to 75°C. Human 26S was not any longer protected from inhibition when treated with NMR lysate exposed to temperatures higher than 45°C (Figure 4D). We envisioned two possible scenarios: a) that multiple proteins present in high levels in naked mole-rat but not in mouse cytosols create an environment generally supporting activation and resistance, or that b) the naked mole-rat cytosol contains a specific protein or a protein complex that interacts with the proteasome, commanding its activation and resistance.

In an attempt to identify the components of the SN_{NMR} that confer inhibition resistance, the 5-hr supernatant was fractionated by gel filtration chromatography. $Prot_{NMR}$ was added to each chromatographic fraction and ChT-L activity was measured in the presence or absence of the MG132 proteasome inhibitor. The presence of a distinct macromolecular resistance factor particle would be evident if only one or a few fractions convey the resistance. The total loss of protective capabilities after the cytosol fractionation would suggest that macromolecular resistance factor is not stable to gel filtration conditions or that the cytosolic

environment in general is responsible for the protection. The potential factor(s) conveying inhibition resistance were localized to only two adjacent chromatographic fractions (fr.22 and fr.23) corresponding to relative molecular mass of about 100kDa – 160 kDa (Figure 5A,C). These two fractions were pooled, collectively called fr.23, and used in subsequent experiments. Purified human 26S proteasomes treated with fr.23 were clearly resistant to inhibition when challenged with 10nM BZ (Figure 5B). Therefore, we concluded that the resistance factor present in fr.23 is a stable macromolecule, capable of withstanding the purification procedure, and whose actions on the proteasome can be transferred to other species.

Interestingly, studies examining changes in gene expression in response to MG132 treatment, reveal overlapping features with the heat shock response signaling pathway (30). As such, compounds or pathways that stimulate or maintain chaperone response could also aid in the preservation of proteasome function and recognition of damaged substrates. Western blot analyses revealed that expression levels of three key chaperones, HSP72, HSP40, and HSP25 were significantly higher in naked mole-rat liver cytosolic fractions and 5-hr supernatants than in respective mouse samples (Figure 6A,B; Figure S1). The high levels of these HSPs in naked mole-rats concur with the previously described strong correlation between levels of molecular chaperones and species longevity in reptiles, birds, and mammals (31,32). Cytosolic abundance of these key HSPs in naked mole-rat tissues may contribute to enhanced protection at the molecular, cellular, and whole animal level against the many potential stressors these subterranean-dwelling rodents encounter over the course of their lifespan, and may be responsible for providing a protective intracellular resistant environment. Mass spectrometry analysis of the fr.22 and fr.23 content, the chromatographic fractions conferring inhibition resistance, revealed the presence of naked mole-rat HSP72 (inducible heat shock protein 70, Table 3; Figure S2; See also Supplementary Material Table S1). Consistently, Western blot analyses detected a high level of HSP72 in fr.21, fr.22, and fr.23. HSP40 was also present (Figure 6C) in these fractions. Although HSP25 was the most abundant HSP in the cytosol and 5-hr supernatants (Figure 6A,B), this particular HSP was not found in fr.21–23 but only in the supernatant fraction (SN) (Figure 6C).

3.4 Functional role for HSP72 and HSP40 in the naked mole-rat activation/resistance factor

We next set to test which HSPs contributed to the observed cytosolic protective and regulatory effects on proteasomes by using neutralizing antibodies for HSP40, HSP72, or HSP90. Only anti-HSP70/72 and anti-HSP40 altered sensitivity to inhibition (Figure 7). With increasing concentration of anti-HSP72, activity of proteasome was also reduced (Figure 8A,B). Since mass spectrometry revealed the presence of HSP90 in fr.23 (Table 3), we also tested the influence of specific anti-HSP90 antibodies on proteasomes. This treatment had no effect on inhibition resistance, nor did HSP90 co-precipitate with HSP72 in naked mole-rat lysates (Figure 7C,E). Collectively, these results confirm a key role for the canonical chaperone HSP72, and its co-chaperone HSP40 in the protection of naked mole-rat proteasome function.

To gain insight into the mode of action of the chaperones we challenged HSP72 with two distinct inhibitors: pifithrin-μ (33) and VER155008 (34). Pifithrin-μ, like the neutralizing antibody, binds to the substrate-binding domain of HSP72 (33,35) whereas VER155008 binds to the ATPase domain of HSP72 and prevents ATP hydrolysis (34). Intriguingly, only pifithrin-μ lessened both the inhibition resistance and the increased proteasome activity associated with the SN_{NMR} (Figure 7D; Figure 9). To the contrary, VER155008 had no effect upon sensitivity to inhibition or activity (Figure 10). Divergent responses to pifithrin-μ and VER155008 suggest that the resistance/activation factor function is independent on ATP hydrolysis, but possibly relies on the substrate-binding domain of HSP72. Immunoprecipitation experiments revealed that HSP72 was associated with both the 26S proteasome and HSP40 (Figure 7E), indicating direct interactions between this factor and proteasome in naked mole-rats, and suggesting a critical role of the HSP72/HSP40 co-chaperone relationship for the observed functions of increased proteasome activity and inhibition resistance for this cytosolic factor.

The potential actions of HSP72 and HSP40, as described above, differ markedly from the well-established roles of these molecular chaperones in proteostasis. HSP72 and HSP40 are known to participate in chaperone mediated autophagy [CMA], protein refolding, the prevention of protein aggregation as well as the unfolding and transport of damaged proteins for proteasome-mediated degradation (36). Moreover, it is well known that HSP40 commonly co-localizes with HSP72, and that HSP40 regulates ATP-dependent HSP72 activity (37). However, no HSP has been previously shown to stimulate proteasome activity or for that matter any other protease. A previous study has shown that increased expression of HSP40 (Hdj1) can confer proteasome resistance to inhibition after exposure to oxidative stress in an *in vitro* cell system (38), which supports our *in vivo* findings. Nevertheless, such findings, that HSPs protect the proteasome (or any other protease) from endogenous or environmental stressors or, even more surprisingly, from the various well-documented proteasome-specific competitive inhibitors that induce their inhibition using different mechanisms of action, in a natural animal has not been documented. Moreover, the role of these HSPs in proteasome modulation and protection from inhibition is independent of ATP, further alluding to a previously undocumented novel mechanism for HSP72 action. The C-terminus sequence of NMR and mouse HSP72 show several areas of weaker homology including deletion of a 16 residue long C-terminal peptide in NMR (Figure S3). Since C-terminal part of HSp 72 is responsible for interaction with substrates and Hsp40, such differences may point at alternate binding partners or different efficiency of substrate binding. Interestingly, a strong presence of retinal dehydrogenase was detected in fractions 22 and 23 (Table S1). Although its detection may be simply result of an abundance of the enzyme, it might also be possible that changes in redox status of NADH may play a key role in activating this chaperone response. This possibility is supported by recent finding that NADH binds to the 26S proteasome without ATP (39) and so could be a part of a larger chaperone-proteasome complex.

Despite the fact that mouse cytosolic lysates contain many of the homologous HSPs, albeit at lower concentrations than those found in the naked mole-rat supernatant, they do not appear to convey any of the proteasome protective properties observed in the naked mole-rat cytosol. This is apparent even when the cytosolic lysates are concentrated, with the

exception of a modest activation at the highest concentrations of SN_{MS} used (Figure 4A). It is possible that other macromolecules also contribute to the unique properties of this naked mole-rat cytosolic factor and that this likely forms a complex with the proteasome.

3.5 Morphometric characterization of a complex between 20S proteasome and the resistance factor

Finally, we used atomic force microscopy [AFM], a nondestructive imaging technology capable of detecting the topography of single native biomacromolecule to see if we could identify distinct complexes of purified human 20S proteasome with the resistance factor present in fr. 23 (Figure 11). As previously found with AFM, the tube-shaped human 20S proteasomes bound to a mica surface in two orientations, “standing” (the majority) and “lying” (24). AFM imaging rendered the standing particles as round cone shaped objects (Figure 11B top row). A small fraction of the 20S proteasomes lay on their side and they were observed as rectangular or slightly oval particles (Figure 11B middle row). AFM images of fr. 23 presented as expected a complex mixture of particles of different sizes that were smaller than proteasomes and devoid of large complexes or aggregates (Figure 11A insert). Following the mixing of purified human 20S proteasomes with the naked mole-rat supernatant fr. 23, AFM produced images of a heterogenous mixture of particles. To determine if the mixture contains a new class of particles besides those found separately in fr. 23 and in the purified 20S proteasome preparation, we performed morphometric analysis of images collected for each investigated case followed by hierarchical cluster analysis. We found that about 5% of the particles in the fr. 23 + 20S proteasome mixture was classified as a distinct new population of elongated (33nm long and 10nm wide) objects (Figure 11A; Figure 11B bottom row). At the same time slightly lower abundance of free proteasomes was also observed. Since we could not consistently find any other larger or uniquely shaped molecules in the mixture or changes in object abundance, the identified particles most likely correspond to complexes of the resistance factor with the core proteasome. The dimensions of the complex may imply that the resistance factor binds to the α ring of 20S proteasome since the length of side view proteasome alone is 15–18 nm (31). Furthermore, the topography of identified complexes indicated that both α faces were saturated with the resistance factor. Likely, half saturated complexes also existed but could have been obscured in the morphometric analyses of AFM images by the presence of other similarly sized protein particles in fr. 23. These exciting data support our premise that the cytosolic factor complexes with proteasomes and thereby both modulates their activity and protects them from inhibiting agents.

4. CONCLUSIONS

Clearly, the preternaturally long-lived naked mole-rats have evolved certain molecular mechanisms that contribute to their ability to prolong good health and attenuate the aging process (1). The high proteasome content coupled with its distinctive composition in naked mole-rats, that we previously described may play an integral role in this regard (18). However, we describe here another important, complementary mechanism. We report here for the first time that naked mole-rats express high levels of key chaperones, HSP72, HSP40, and HSP25 even in untreated tissues when compared to those of the mouse. Further we

present evidence suggesting the presence of a novel cytosolic factor that contains two of these chaperones, and that not only protects proteasome function against cell stressors but also enhances proteasome performance. This factor may be a common constitutive feature of long-lived species, or possibly may be induced under specific stress conditions in both naked mole-rats and other organisms. Our finding of a transferable stable factor that protects a critical intracellular proteolytic system may have profound therapeutic significance. We envision that this may guard against the many age-related diseases linked to a dysfunction in proteostasis and the concomitant accrual of protein aggregates, such as occurs in Alzheimer's and Parkinson's diseases. This cytosolic factor may also ameliorate the well-documented decrease in proteasome activity with age (13,14,40,41) and if used therapeutically may thus promote prolonged healthspan and longevity in our own aging population.

Supplementary Material

Refer to Web version on PubMed Central for supplementary material.

Acknowledgments

We thank Drs. Steve Austad, James Nelson and Shane Rea for their constructive criticism of the earlier versions of this manuscript; Kaitlyn Lewis, Megan Smith and the LAR at UTHSCSA who were responsible for the care and maintenance of the naked mole-rat colony. Mass spectrometry analyses were conducted in the UTHSCSA Institutional Mass Spectrometry Laboratory by Kevin W. Hakala and Sam Pardo. KAR was supported by a Training Grant through the NIH/NIA (T32 AG021890) and an American Federation for Aging Research (AFAR)/Ellison Postdoctoral Fellowship to continue this work under the mentorship of RB. This work was also funded by awards to RB from the NIH/NIA (1R21AG043912), Glenn Foundation, the Ellison Medical Foundation and Breakthroughs in Gerontology from the AFAR.

Abbreviations

Adh(VS)	adamantane-acetyl-(6-aminohexanoyl)$_3$-(leucinyl)$_3$-vinyl-(methyl)-sulfone
BZ	bortezomib
ChTL	chymotrypsin-like
FT	filtrate
HSP	heat shock protein
IC_{50}	concentration required to ablate 50% of activity
LC	lactacystin
PRS_{MS}	mouse partially-purified proteasome 5h pellet
SN_{Ms}	mouse supernate MG132, N-(benzyl-oxycarbonyl) leucinyl-leucinal
NMR	naked mole-rat
PRS_{NMR}	NMR partially-purified proteasome 5h pellet
SN_{NMR}	NMR supernate
PGPH	post-glutamyl peptide hydrolyzing

PRS	proteasome
RT	retentate
SN	supernate
TL	trypsin-like
Ub	ubiquitin
UPS	ubiquitin proteasome system

References

1. Buffenstein R. Negligible senescence in the longest living rodent, the naked mole-rat: insights from a successfully aging species. J Comp Physiol B. 2008; 178:439–445. [PubMed: 18180931]
2. Andziak B, Buffenstein R. Disparate patterns of age-related changes in lipid peroxidation in long-lived naked mole-rats and shorter-lived mice. Aging Cell. 2006; 5:525–532. [PubMed: 17129214]
3. Buffenstein R. The naked mole-rat; a new long-living model for human aging research. J Gerontol Biol Sci. 2005; 60:1369–1377.
4. Salmon AB, Akha AAS, Buffenstein R, Miller RA. Fibroblasts from naked mole-rats are resistant to multiple forms of cell injury, but sensitive to peroxide, ultraviolet light, and endoplasmic reticulum stress. J Ger Biol Sci Med Sci. 2008; 63:232–241.
5. Lewis KN, Mele J, Hornsby PJ, Buffenstein R. Stress Resistance in the Naked Mole-Rat: The Bare Essentials - A Mini-Review. Gerontology. 2012; 58:453–462. [PubMed: 22572398]
6. Pérez VI, Buffenstein R, Masamsetti V, Leonard S, Salmon AB, Mele J, Andziak B, Yang T, Edrey YH, Friguet B, Ward W, Richardson A, Chaudhuri A. Protein stability and resistance to oxidative stress are determinants of longevity in the longest-living rodent, the naked mole-rat. Proc Natl Acad Sci USA. 2009; 106:3059–3064. [PubMed: 19223593]
7. Morimoto RI, Cuervo AM. Protein Homeostasis and Aging: Taking Care of Proteins From the Cradle to the Grave. J Ger Biol Sci Med Sci. 2009; 64:167–170.
8. Balch WE, Morimoto RI, Dillin A, Kelly JW. Adapting proteostasis for disease intervention. Science. 2008; 319:916–919. [PubMed: 18276881]
9. Grimm S, Hohn A, Grune T. Oxidative protein damage and the proteasome. Amino acids. 2012; 42:23–38. [PubMed: 20556625]
10. Hanna J, Finley D. A proteasome for all occasions. FEBS Lett. 2007; 581:2854–2861. [PubMed: 17418826]
11. Zwickl P, Seemuller E, Kapelari B, Baumeister W. The proteasome: a supramolecular assembly designed for controlled proteolysis. Adv Protein Chem. 2001; 59:187–222. [PubMed: 11868272]
12. Jung T, Grune T. The proteasome and its role in the degradation of oxidized proteins. IUBMB Life. 2008; 60:743–752. [PubMed: 18636510]
13. Rodriguez KA, Gaczynska M, Osmulski PA. Molecular mechanisms of proteasome plasticity in aging. Mech Ageing Dev. 2010; 131:144–155. [PubMed: 20080121]
14. Ferrington DA, Husom AD, Thompson LV. Altered proteasome structure, function, and oxidation in aged muscle. FASEB J. 2005; 19:644–646. [PubMed: 15677694]
15. Chondrogianni N, Petropoulos I, Franceschi C, Friguet B, Gonos ES. Fibroblast cultures from healthy centenarians have an active proteasome. Exp Gerontol. 2000; 35:721–728. [PubMed: 11053662]
16. Kim EB, Fang X, Fushan AA, Huang Z, Lobanov AV, Han L, Marino SM, Sun X, Turanov AA, Yang P, Yim SH, Zhao X, Kasaikina MV, Stoletzki N, Peng C, Polak PXZ, Kiezun A, Zhu Y, Chen Y, Kryukov GV, Zhang Q, Peshkin L, Yang L, Bronson RT, Buffenstein R, Wang B, Han C, Li Q, Chen L, Zhao W, Sunyaev SR, Park TJ, Zhang G, Wang J, Gladyshev VN. Genome sequencing reveals insights into physiology and longevity of the naked mole rat. Nature. 2011; 479:223–227. [PubMed: 21993625]

17. Yu C, Li Y, Holmes A, Szafranski K, Faulkes CG, Coen CW, Buffenstein R, Platzer M, de Magalhaes JP, Church GM. RNA sequencing reveals differential expression of mitochondrial and oxidation reduction genes in the long-lived naked mole-rat when compared to mice. PLoS One. 2011; 6:e26729. [PubMed: 22073188]
18. Rodriguez KA, Edrey YH, Osmulski P, Gaczynska M, Buffenstein R. Altered composition of liver proteasome assemblies contributes to enhanced proteasome activity in the exceptionally long-lived naked mole-rat. PLoS One. 2012; 7:e35890. [PubMed: 22567116]
19. Lewis KN, Andziak B, Yang T, Buffenstein R. The Naked Mole-rat Response to Oxidative Stress: Just Deal With it. Antioxid Redox Signal. 2012; 19:1388–1399. [PubMed: 23025341]
20. Pickering AM, Davies KJ. Differential roles of proteasome and immunoproteasome regulators Pa28alphabeta, Pa28gamma and Pa200 in the degradation of oxidized proteins. Arch Biochem Biophys. 2012; 523:181–190. [PubMed: 22564544]
21. Pinto M, Jepsen KJ, Terranova CJ, Buffenstein R. Lack of sexual dimorphism in femora of the eusocial and hypogonadic naked mole-rat: a novel animal model for the study of delayed puberty on the skeletal system. Bone. 2010; 46:112–120. [PubMed: 19761882]
22. Cvek B, Dvorak Z. The ubiquitin-proteasome system (UPS) and the mechanism of action of bortezomib. Current pharmaceutical design. 2011; 17:1483–1499. [PubMed: 21504411]
23. Kisselev AF, Callard A, Goldberg AL. Importance of the different proteolytic sites of the proteasome and the efficacy of inhibitors varies with the protein substrate. J Biol Chem. 2006; 281:8582–8590. [PubMed: 16455650]
24. Gaczynska M, Osmulski PA. Atomic force microscopy of proteasome assemblies. Methods Mol Biol. 2011; 736:117–132. [PubMed: 21660725]
25. Kessler BM, Tortorella D, Altun M, Kisselev AF, Fiebiger E, Hekking BG, Ploegh HL, Overkleeft HS. Extended peptide-based inhibitors efficiently target the proteasome and reveal overlapping specificities of the catalytic beta-subunits. Chemistry & biology. 2001; 8:913–929. [PubMed: 11564559]
26. de Bettignies G, Coux O. Proteasome inhibitors: Dozens of molecules and still counting. Biochimie. 2010; 92:1530–1545. [PubMed: 20615448]
27. Orlowski RZ, Kuhn DJ. Proteasome inhibitors in cancer therapy: lessons from the first decade. Clinical cancer research : an official journal of the American Association for Cancer Research. 2008; 14:1649–1657. [PubMed: 18347166]
28. Gaczynska M, Rock KL, Goldberg AL. Gamma-Interferon and Expression of MHC Genes Regulate Peptide Hydrolysis by Proteasomes. Nature. 1993; 365:264–267. [PubMed: 8396732]
29. Cascio P, Goldberg AL. Preparation of hybrid (19S-20S-PA28) proteasome complexes and analysis of peptides generated during protein degradation. Methods Enzymol. 2005; 398:336–352. [PubMed: 16275341]
30. Kim HJ, Joo HJ, Kim YH, Ahn S, Chang J, Hwang KB, Lee DH, Lee KJ. Systemic analysis of heat shock response induced by heat shock and a proteasome inhibitor MG132. PLoS One. 2011; 6:e20252. [PubMed: 21738571]
31. Salway KD, Gallagher EJ, Page MM, Stuart JA. Higher levels of heat shock proteins in longer-lived mammals and birds. Mech Ageing Dev. 2011; 132:287–297. [PubMed: 21703294]
32. Krivoruchko A, Storey KB. Forever young: mechanisms of natural anoxia tolerance and potential links to longevity. Oxidative medicine and cellular longevity. 2010; 3:186–198. [PubMed: 20716943]
33. Leu JI, Pimkina J, Frank A, Murphy ME, George DL. A small molecule inhibitor of inducible heat shock protein 70. Mol Cell. 2009; 36:15–27. [PubMed: 19818706]
34. Massey AJ, Williamson DS, Browne H, Murray JB, Dokurno P, Shaw T, Macias AT, Daniels Z, Geoffroy S, Dopson M, Lavan P, Matassova N, Francis GL, Graham CJ, Parsons R, Wang Y, Padfield A, Comer M, Drysdale MJ, Wood M. A novel, small molecule inhibitor of Hsc70/Hsp70 potentiates Hsp90 inhibitor induced apoptosis in HCT116 colon carcinoma cells. Cancer chemotherapy and pharmacology. 2010; 66:535–545. [PubMed: 20012863]
35. Dehghani M, Xiao CF, Money TGA, Shoemaker KL, Robertson RM. Protein expression following heat shock in the nervous system of Locusta migratoria. Journal of Insect Physiology. 2011; 57:1480–1488. [PubMed: 21855549]

36. Rampelt H, Kirstein-Miles J, Nillegoda NB, Chi K, Scholz SR, Morimoto RI, Bukau B. Metazoan Hsp70 machines use Hsp110 to power protein disaggregation. EMBO J. 2012; 31:4221–4235. [PubMed: 22990239]

37. Fan CY, Lee S, Cyr DM. Mechanisms for regulation of Hsp70 function by Hsp40. Cell Stress Chaperones. 2003; 8:309–316. [PubMed: 15115283]

38. Ding Q, Keller JN. Proteasome inhibition in oxidative stress neurotoxicity: implications for heat shock proteins. J Neurochem. 2001; 77:1010–1017. [PubMed: 11359866]

39. Tsvetkov P, Myers N, Eliav R, Adamovich Y, Hagai T, Adler J, Navon A, Shaul Y. NADH Binds and Stabilizes the 26S Proteasomes Independent of ATP. J Biol Chem. 2014; 289:11272–11281. [PubMed: 24596095]

40. Dasuri K, Nguyen A, Zhang L, Fernandez-Kim SO, Bruce-Keller AJ, Blaloc BA, deCabo R, Keller JN. Comparison of Liver and Brain Proteasomes for Oxidative Stress Induced Inactivation: Influence of Aging and Dietary Restriction. Free Rad Res. 2009; 43:28–36.

41. Dasuri K, Zhang L, Ebenezer P, Fernandez-Kim SO, Bruce-Keller AJ, Szweda LI, Keller JN. Proteasome alterations during adipose differentiation and aging: links to impaired adipocyte differentiation and development of oxidative stress. Free Radic Biol Med. 2011; 51:1727–1735. [PubMed: 21871954]

Highlights

- The naked mole-rat proteasome is protected from inhibition
- This is accomplished by a transferable chaperone-containing cytosolic factor.
- The factor interacts with naked mole-rat proteasome enhancing its activity.
- This factor protects and increases proteasome function of widely divergent species.
- The factor participates in a novel mechanism that may help to defy cellular aging.

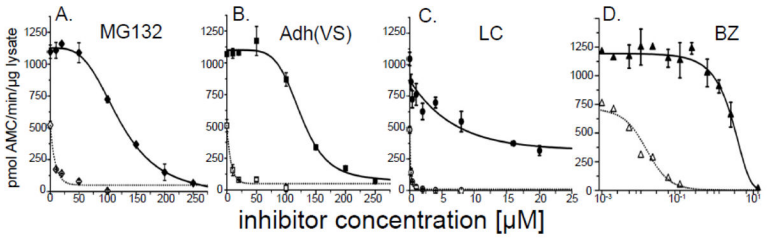

FIGURE 1. Proteasomes from naked mole-rat [NMR] cytosol show resistance to proteasome specific competitive inhibitors

Dramatically different ChT-L activity was evident in response to increasing concentrations of inhibitors representing four different classes of the compounds: (**A**) an aldehyde, MG132; (**B**) a vinyl sulfone, Adh(VS); (**C**), a lactone, LC and (**D**) a boronate, BZ. To compare the inhibition resistance between NMR (solid symbols) and mouse (open symbols), we calculated the IC_{50} value, which corresponds to the concentration of inhibitor required to ablate 50% of activity. The IC_{50} for (A) MG132 was 15X, (B) Adh(VS) 18x, (C) LC 40x, and (D) BZ 163x greater in NMR samples compared to those of mice. See also Table 1 for IC_{50} values. Calculations are based on ChT-L activity assessments from lysates of at least 3 mice or 6 NMRs.

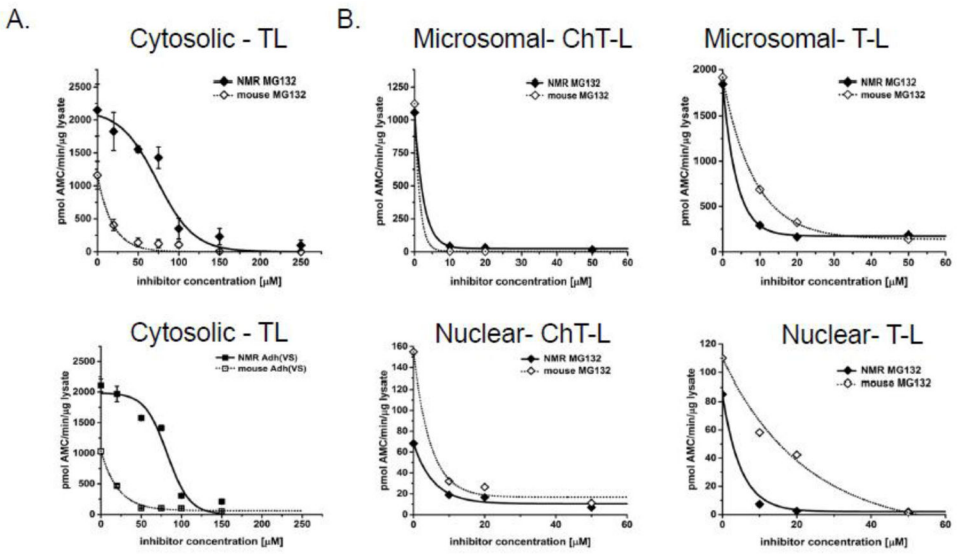

FIGURE 2. Trypsin-like activity of proteasome in NMR cytosolic fractions was more resistant to competitive inhibitors than mouse proteasome, although less profoundly than the ChT-L activity. However, resistance was not observed in the microsomal or nuclear fractions of either species

(A) Based on IC_{50} values, the proteasome in NMR cytosol is about 5 times less susceptible to both MG132 (top) and Adh(VS) (bottom) than was the mouse cytosol. See also Table 1.

(B) In contrast, no significant differences in inhibitor resistance between NMR and Ms were found in the microsomal or nuclear fractions as tested with MG132. See also Table 1.

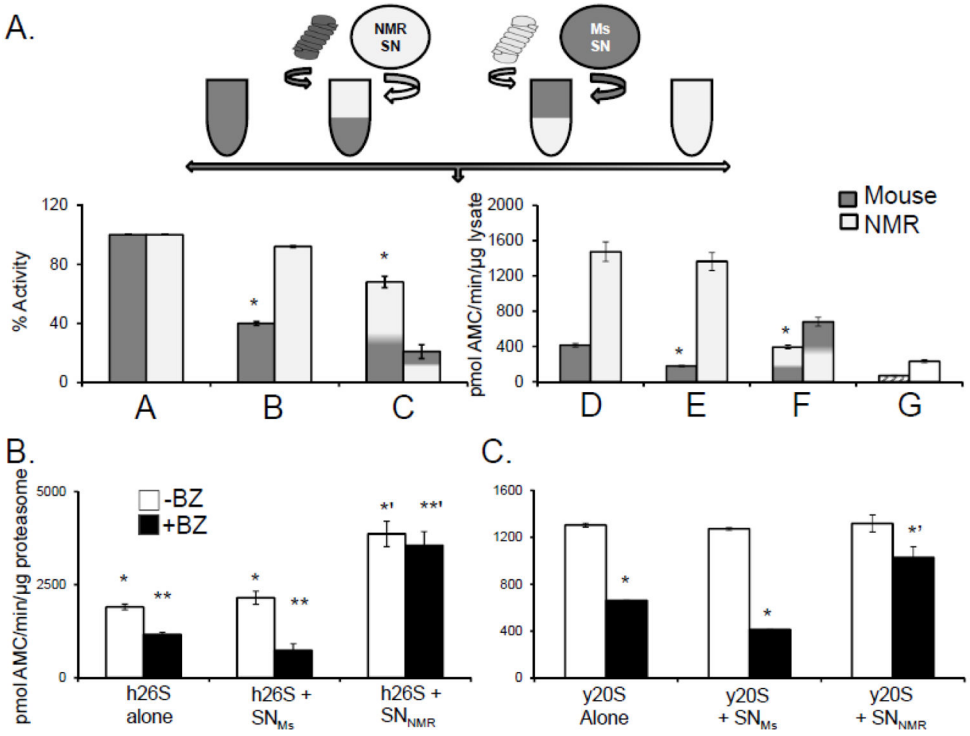

FIGURE 3. An NMR cytosolic factor confers resistance to mammalian and yeast proteasomes from competitive inhibition

(A) *Top panel:* Schematic showing the design of the cross over experiment set up to evaluate if species differences in proteasome resistance to inhibition reflect an intrinsic property of the proteasome or the presence of a protective cytosolic factor. See Crossover Assays in Methods below for details. *Bottom panel*: When $Prot_{Ms}$ were resuspended in SN_{NMR} they showed elevated activity and inhibition resistance, whereas $Prot_{NMR}$ exposed to SN_{MS} displayed both lower activity and greater sensitivity to inhibition. Bars A and D represents the activity of reconstituted MS and NMR cytosols (A = percentage set to 100% activity and D= ChT-L activity per mg lysate) in the absence of any inhibitor. B and E reveal the change in activity following treatment of the reconstituted cytosols with 20 µM MG132 and indicate that in comparison with mouse, the proteasome in NMR cytosol is resistant to inhibition. Bars C and F demonstrate that when $Prot_{Ms}$ were resuspended in SN_{NMR} they exhibited elevated activity and acquired inhibition resistance ($p<0.05$), whereas $Prot_{NMR}$ resuspended in SN_{Ms} showed both lower activity and greater sensitivity to inhibition ($p<0.05$) (means ± S.E.M.; n =5). Bar G reveals that the SN alone had very low peptidolytic activity. **(B)** Human 26S proteasomes [h26S] treated with SN_{NMR}, but not SN_{Ms} or buffer, showed increased ChT-L activity (solid bars) and pronounced resistance to 10nM BZ (hatched bars) (* to *', $p<0.003$; ** to **', $p<0.0004$; means ± S.E.M; n = 6). **(C)** SN_{NMR} conveyed inhibition resistance to the yeast proteasome [y20S]. SN_{MS} did not show this effect. No significant increase in activity in the presence of SN_{NMR} was detected. (* and ** indicated $p < 0.01$; means ± S.E.M.; n = 3)

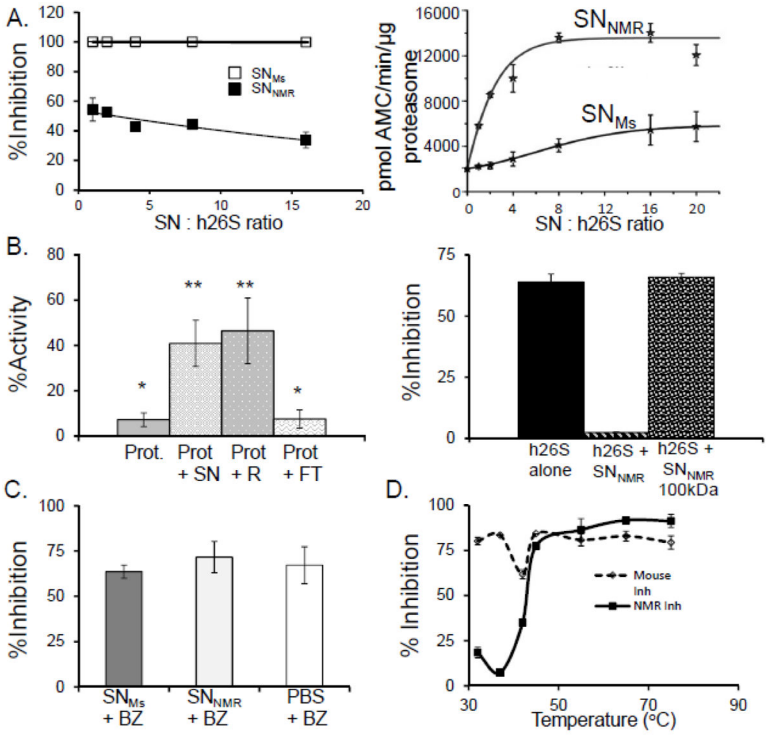

FIGURE 4. NMR cytosol contains a protein factor conveying resistance to inhibition and leading to activation of the proteasome

(A) Titration of human 26S proteasome [h26S] with increasing protein concentration of mouse supernatant [SN_{MS}] (open squares) did not result in acquiring resistance to inhibition with 20 μM MG132 even at 16-fold excess of SN_{MS}. In contrast, resistance was evident even at lowest used SN_{NMR}: h26S ratio (1:1, 250ng of each component), and was slightly stronger with increasing SN_{NMR}: h26S ratio (left panel; closed squares). Chymotrypsin-like [ChT-L] activity of h26S was rapidly and profoundly enhanced by the addition of SN_{NMR}, reaching a plateau with more than 6-fold activation at about 8:1 (SN_{NMR}: h26S) ratio (right panel). However, treatment with the 8-fold excess of SN_{MS} resulted in only 2-fold activation of h26S, and the activation never exceeded 3-fold under the conditions used (n =5). (B) SN_{NMR} was fractionated with a spin filter with 3,000 Da pore cutoff membrane (top panel) or with a 100,000 Da pore cutoff membrane (bottom panel). Top panel demonstrates ChT-L activities of $Prot_{NMR}$ after treatment with 20 μM MG132, alone or with addition of the whole SN_{NMR}, the 3,000 Da retentate (R_{NMR}; molecules with apparent molecular weights higher than 3,000 Da) or the 3,000 Da filtrate [FT_{NMR}; molecules with apparent molecular weights lower than 3,000 Da]. The activity of inhibitor-challenged $Prot_{NMR}$ was markedly higher after treatment with the whole SN_{NMR} (compare with Fig. 2A, bottom panel) or with the R_{NMR}, but not with FT_{NMR}. Spin-filtering the SN_{NMR} through a 100,000 Da pore cutoff membrane, and performing the ChT-L activity assay with h26S treated with 20μM of MG132 (left bar) the inhibition resistance was conveyed by the SN_{NMR} (middle bar; compare with Fig. 2B) but not by the filtrate (right bar; MW>100,000 Da, n =5 each treatment). (C) The ChT-L activity of h26S proteasome was markedly inhibited by all three filtrates, indicating that BZ was not significantly sequestered by SN_{NMR}, as compared with SN_{Ms} or buffer (n = 6). (D) To test if the factor is heat liable we subjected SN_{NMR} and SN_{Ms}

to heat stress at temperatures ranging from 32°C to 75°C. The heat-treated SNs were then added to h26S and ChT-L proteasome activity and inhibition resistance were assessed with 10nM BZ. Heat-treatment above 45°C ablated the inhibition resistance conveyed by SN_{NMR} strongly suggesting a protein nature of the proteasome-affecting factor (n = 5).

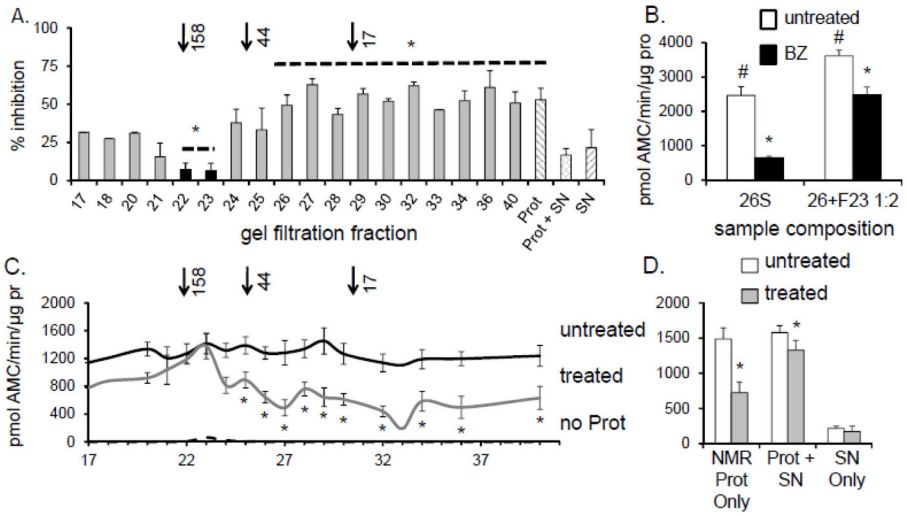

FIGURE 5. NMR proteasome resistance to inhibition was found in two gel filtration fractions

Proteasome-depleted SN_{NMR} was fractionated by gel filtration. **(A)** $Prot_{NMR}$ was added to the gel filtration fractions and proteasome-specific inhibition resistance was measured after treatment of each fraction with 20 μM MG132. Only fractions 22 and 23 consistently protected the $Prot_{NMR}$ ChT-L activity from MG132 inhibition (*$p<0.05$; mean ± S.E.M., n = 5). Although fr.21 contained HSP72 and HSP 40 it did not confer significant inhibition resistance. Arrows above A indicate elution of the molecular weight standards. **(B)** ChT-L activity (expressed per mg protein, [pro]) of human 26S proteasome [h26S] was significantly increased and protected from inhibition by 10 nM BZ when suspended in the resistance factor-enriched fr.23 (#$p<0.01$, *$p<0.0004$). Treatment with 10 nM BZ ablated activity of h26S by 75%. In the presence of fr. 23 ChT-L activity of h26S exposed to BZ was reduced only by 30%. **(C)** Naked mole-rat [NMR] proteasome-enriched pellet [$Prot_{NMR}$] was added to the gel filtration fractions and chymotrypsin-like [ChT-L] activity was measured after treatment with 20μM, MG132 (“treated”) or DMSO vehicle (“untreated”). Essentially no ChT-L activity was detected in the fractions in the absence of $Prot_{NMR}$ (“no Prot”). (*$p<0.05$; mean ± S.E.M.; n = 5). Only $Prot_{NMR}$ added to fractions 22 and 23 was refractory to MG132. **(D)** $Prot_{NMR}$ alone was sensitive to MG132 inhibition, unlike $Prot_{NMR}$ re-suspended in SN_{NMR} (*$p < 0.02$). Very low peptidolytic activity was detected in SN_{NMR} (see also C, hashed columns).

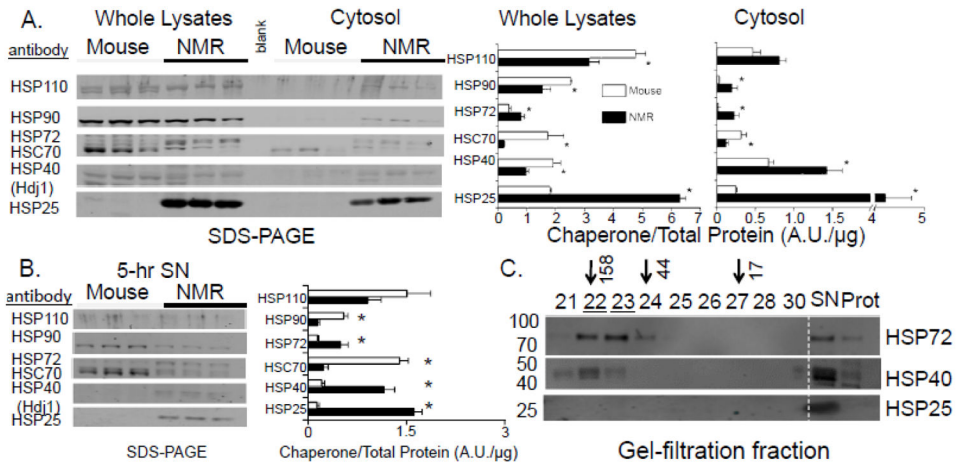

FIGURE 6. NMR showed higher levels of majority of cytosolic HSPs than did mice (A, B). On the other hand, gel filtration fractions influencing PRS resistance contained only high levels of HSP72 and HSP40 (C)

(A) Multiplex Western blots of whole lysates and cytosolic preparations and their quantification (bar graphs) after standardization to total protein (Ponceau-S, see Figure S1) showed dramatic species differences in relative content of HSP90, HSP72, HSC70, HSP40, and HSP25. Mean values and standard error bars are shown (*$p<0.005$). (B) 5-hr SNs showed similar differences in HSPs content to that of the cytosolic preparations. (C) As demonstrated by Western blotting (left, molecular weights), $SN_{NMR,}$ fr.22, and fr.23 (underlined) contained high levels of HSP72, some HSP40, and virtually no HSP25. Arrows indicate elution of the molecular weight standards and numbers on the left of the figure represent molecular weights.

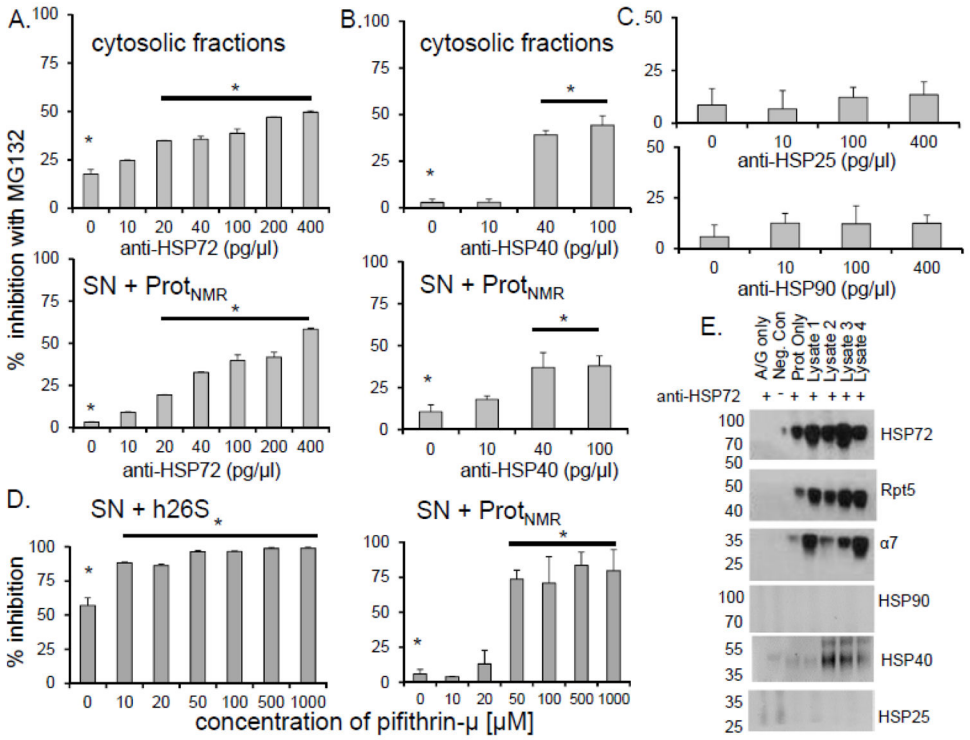

FIGURE 7. HSP72 and HSP40 played a critical role in inhibition resistance of naked mole-rat proteasomes

(A, B) Titration of the naked mole-rat cytosolic fraction and SN_{NMR} with increasing amounts of neutralizing antibodies against HSP72 and HSP40 significantly decreased the level of inhibition resistance (*p<0.001) (mean ± S.E.M., n = 6). **(C)** Anti-HSP25 or anti-HSP90 did not affect sensitivity to inhibition. **(D)** Treatment with increasing concentrations of the HSP72-specific inhibitor pifithrin-µ attenuated resistance to inhibition (*p<0.01) (mean ± S.E.M., n = 5). **(E)** Immunoprecipitation with anti-HSP70/72 antibody showed interaction between HSP72 and the NMR 26S (α7, Rpt5) as well as with HSP40, but not with HSP25 or HSP90.

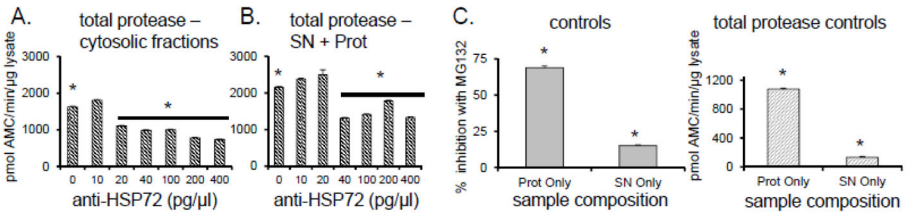

FIGURE 8. HSP72 depletion affects not only inhibition resistance but also peptidase activity of proteasome

(A) Up to 40% decline in ChT-L activity was observed when cytosolic lysates were mixed with at least anti-HSP70/72 antibodies (*p<0.001). (B) A similar decrease of activity with reconstituted naked-mole rat supernatant [SN] and partially purified naked mole-rat proteasomes [Prot] was observed (*p<0.001). (C) NMR proteasome [Prot] in the absence of SN does not exhibit inhibitor resistance (left). Moreover, NMR supernatant [SN] does not present any appreciable ChT-L peptidase activity (right).

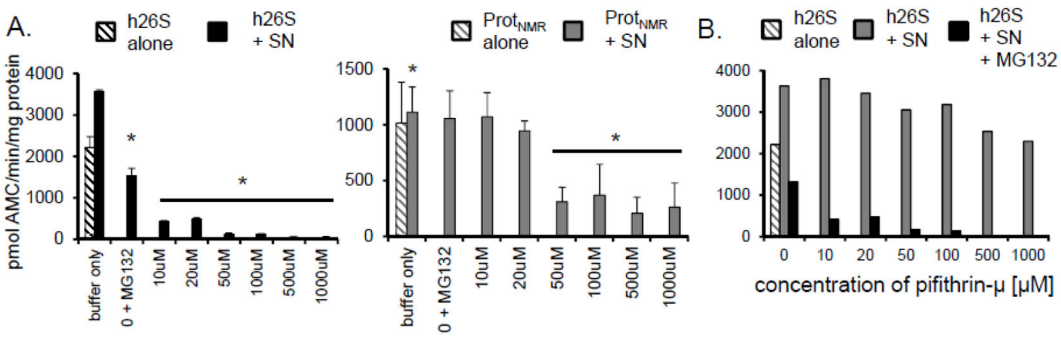

FIGURE 9. Inhibition of Hsp72 in naked mole-rat supernatants [SN_{NMR}] with a specific small-molecule inhibitor pifithrin-μ attenuates the ability to convey resistance in a dose-dependent manner

(A) In both reconstituted naked mole-rat samples (Prot + SN; left panel) and human proteasomes [h26S] resuspended in SN_{NMR} (right panel), and then treated with 20μM MG132, the well-preserved chymotrypsin-like [ChT-L] proteasome activity declined with the addition of increasing concentrations of pifithrin-μ. Significant interference with the inhibition resistance was apparent at the 10μ – 50 μM range of pifithrin-μ concentrations. (B) However, pifithrin-μ did not significantly affect activity of the uninhibited proteasome until much higher concentrations (500 μM). Even then, the activity of pifithrin-μ - treated proteasomes was not lower than activity of the h26S in buffer alone.

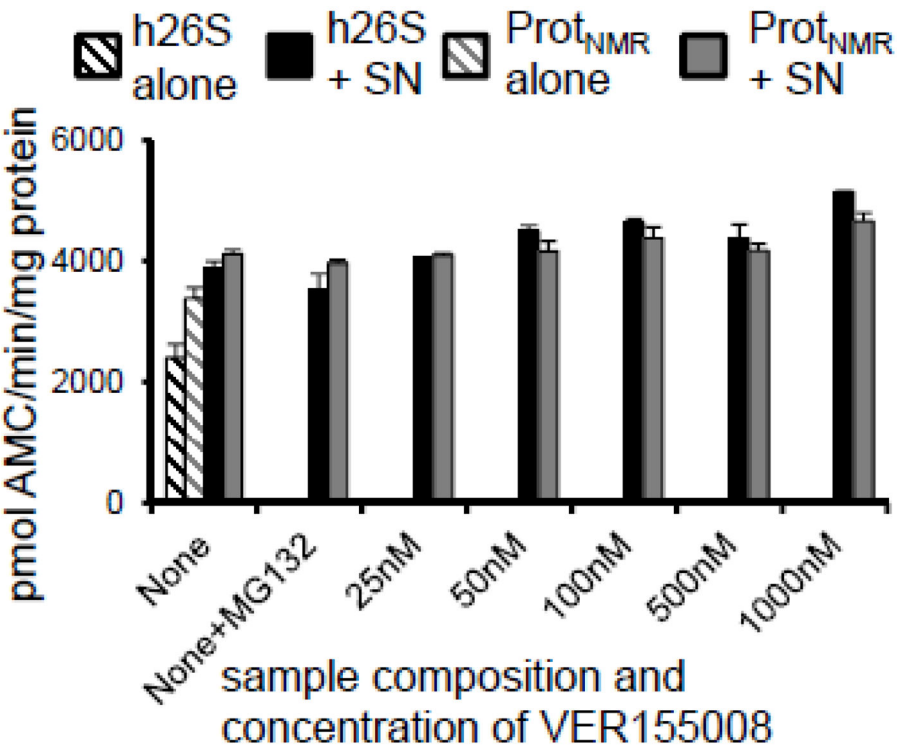

FIGURE 10. The HSP72-specific inhibitor, VER155008, did not affect inhibition resistance

Titration of SN_{NMR} with VER155008 did not disrupt the inhibition resistance of the human or naked mole-rat proteasome challenged with MG132.

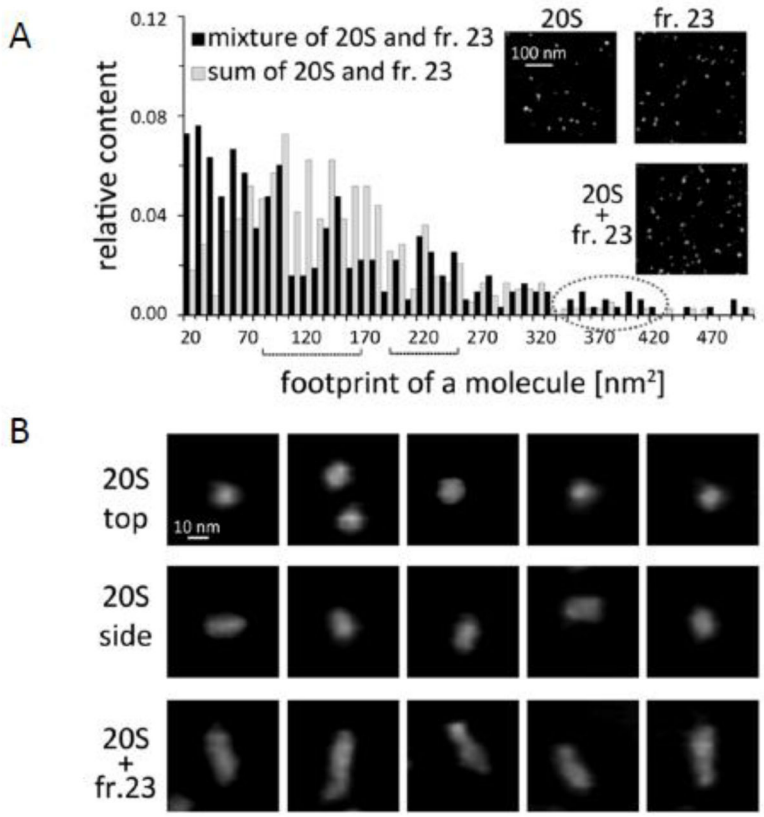

FIGURE 11. Atomic force microscopy [AFM] imaging identified putative complexes between proteasome and resistance factor

(A) Frequency histogram of footprint area of the AFM detected particles in a mixture of purified h20S proteasome with a gel filtration fr. 23 containing resistance factor (black columns) and algebraic sum of the particle counts obtained separately with purified h20S proteasome and fr. 23 (gray columns). Inserts show AFM images of particle fields representing h20S, fr. 23 and their mixture **(B)** A gallery of representative images of particles zoomed-in from the fields of h20S (top-view and side-view) and h20S – fr. 23 mixture. The elongated molecules representing presumed proteasome-resistance factor complexes form the new class of particles, which appeared only when h20S was mixed with fr. 23. Tapping mode in liquid was used to collect height images (see Methods). The grey scale in all AFM images represents height of the particles, with black color corresponding to the background (0 nm) and white color corresponding to 20 nm. A gray dot line oval marks bins comprising a new class of particles present only in the mixture and centered around 360–380 nm^2 (3B, bottom row). Black braces indicate ranges of area sizes characteristic for upright (A, left brace; B top row) and lying side view (A, right brace B middle row) h20S. Between 200 and 300 particles were analyzed for each case. Relative abundance of the new complexes in the mixture was 4.7% and average size of particles was 33x10nm (length x width). Inserts show fragments of AFM images of fields with respective particles.

TABLE 1

NMR proteasome ChT-L and T-L activity only in the cytosolic fraction showed remarkable resistance to competitive inhibition as indicated by significant differences (*, $p > 0.05$) when compared to mouse values. IC_{50} values are indicated in μM ± S.E.

Fraction/Inhibitor	ChT-L IC_{50} (μM)		T-L IC_{50} (μM)	
	NMR	Ms	NMR	Ms
Cytosolic/ Adh (VS)	125.0±5.6*	5.56±1.57*	80.6±2.5*	16.2±1.9*
Cytosolic/ MG132	122.0±5.5*	8.22±2.75*	71.4±8.7*	14.6±4.4*
Cytosolic/LC	6.15±1.4*	0.156±0.005*	--	--
Cytosolic/BZ	2.45±0.74*	0.015±0.004*	--	--
Microsomal/MG132	1.79	0.99	3.01	6.63
Nuclear/ MG132	6.49±2.70	4.6±1.62	2.70±1.4	12.8±4.7

-- = no data; Adh (VS) = adamantane-acetyl-(6-aminohexanoyl)3-(leucinyl)3- vinyl-(methyl)-sulfone ; MG132 = N-(benzyl-oxycarbonyl) leucinyl-leucinyl- leucinal; LC = lactacystin; BZ = bortezomib

TABLE 2

The inhibition resistance factor was associated with high molecular weight molecule(s) that were preserved in a retentate after SN fractionation through a Centricon 3000

Naked mole-rat supernatant [SN], retentate [R], or flow-through [FT] was added to proteasomes [Prot] of both species [$Prot_{NMR}$ or $Prot_{MS}$]. Neither the partially purified proteasomes alone nor the proteasomes mixed with FT showed resistance to inhibition when treated with a range of MG132 concentrations. In contrast, addition of either the SN or R did convey inhibition resistance. These data complement the results presented in Figure 4B, showing expanded concentrations of MG132 tested as well as percent inhibition. Results are presented as pmol AMC/min/μg protein.

conc. MG132 (μM)→	0	10		20		50	
Sample	**Mean ± SE**	**Mean ± SE**	**% Inhibition**	**Mean ± SE**	**% Inhibition**	**Mean ± SE**	**% Inhibition**
$Prot_{NMR}$	514 ± 9	72 ± 13	86.0	43 ± 0.3	91.6	23 ± 1.0	95.5
$Prot_{NMR}$ + SN	1011 ± 15 *#	488 ± 58 *#	51.7	499 ± 71 *#	50.6	327 ± 104 *#	67.7
$Prot_{NMR}$ + R	785 ± 106 *#	542 ± 181 *#	31.0	479 ± 146 *#	39.0	378 ± 104 *#	51.8
$Prot_{NMR}$ + FT	237 ± 45	40 ± 18	83.1	27 ± 18	88.6	16 ± 13	93.2
$Prot_{MS}$	201 ± 1.0	25 ± 0.1	87.6	17 ± 0.2	91.5	11 ± 0.1	94.5
$Prot_{MS}$ + SN	263 ± 2.0 *#	126 ± 22 *#	52.1	116 ± 20 *#	55.9	84 ± 34 *#	68.1
$Prot_{MS}$ + R	282 ± 28 *#	178 ± 72 *#	36.9	172 ± 70 *#	39.0	89 ± 12 *#	68.4
$Prot_{MS}$ + FT	117 ± 13	17 ± 0.3	85.5	15 ± 3.0	87.2	3.0 ± 1.9	97.4

Statistical significance is indicated on the table below (ANOVA,

*p < 0.05 to Prot;

#p < 0.05 to FT).

TABLE 3

Mass spectrometry of fractions 22 and 23 revealed the presence of several molecular chaperones. For a complete list please see also Table S1.

Identified Proteins (8/223)	Accession Number	Molecular Weight	fr.22	fr.23
inducible heat shock protein 70 (HSP72) [Heterocephalus glaber]	gi|13242237 (+26)	71 kDa	28	
Ubiquitin-like modifier-activating enzyme 1 [Heterocephalus glaber]	gi|351699501	119 kDa	20	12
78 kDa glucose-regulated protein [Heterocephalus glaber]	gi|351702099	72 kDa	10	5
inducible heat shock protein 70 [Mus musculus]	gi|118490060 (+7)	70 kDa	8	6
Hsp90aa1 protein [Mus musculus]	gi|118142832 (+23)	66 kDa	8	7
heat shock protein 90 beta [Equus caballus]	gi|12082134 (+17)	82 kDa	7	8
Protein disulfide-isomerase [Heterocephalus glaber]	gi|351706419	57 kDa	7	5
stress-70 protein, mitochondrial [Mus musculus]	gi|162461907 (+9)	73 kDa	7	6

Quantitative value as calculated by the Scaffold v3 program are shown in the table under fr.22 and fr.23 columns.